The Journal of Antibiotics (2019) 72:260–270
https://doi.org/10.1038/s41429-019-0147-2

JARA Japan Antibiotics Research Association
The Society for Actinomycetes Japan

ARTICLE

Design and fabrication of novel thiourea coordination compounds as potent inhibitors of bacterial growth

Sajjad Rakhshani[1] · Ali Reza Rezvani[1] · Michal Dušek[2] · Václav Eigner[2]

Received: 10 October 2018 / Revised: 19 December 2018 / Accepted: 16 January 2019 / Published online: 12 February 2019

Abstract

A new thiourea ligand (**HL**), namely *N*-(4-chlorophenyl)morpholine-4-carbothioamide and its Co(III), Ni(II) and Ag(I) complexes (**1a**, **1b** and **1c**) were synthesized and investigated by Fourier-transform infrared, ^{1}H NMR and UV-visible spectroscopies. The compounds **HL** and **1c** were characterized by single-crystal X-ray crystallography revealing the triclinic space group $P\bar{1}$ for both compounds. The inhibitory effect of **HL** ligand, **1a**, **1b**, and **1c** complexes was investigated with in vitro tests on Gram-positive and Gram-negative bacteria. For the **1c** complex, the results showed that the coordination of the **HL** to Ag(I) ion increased its antibacterial effect especially against *E. coli*. The assays also indicated that for the same bacteria strains, the new complexes showed higher activity than the ligand, with the relative activity **1c > 1b > 1a > HL**. Moreover, all samples were more suitable antimicrobial agents against the Gram-negative than those of the Gram-positive bacteria. Eventually, the relationship between the structure and bactericidal activities of these specimens was examined by calculating frontier molecular orbital (HOMO and LUMO) energies using density functional theory method at the 6-31 G*/LANL2DZ level of theory.

Introduction

Thiourea compounds are important ligands in coordination chemistry, indispensable intermediates for the preparation of organocatalysts or ancillaries in chemosensors, and important part of anticorrosion compounds [1, 2]. They are widely recognized for their biological and antibacterial properties, with increasing use as antitubercular or anti-tumor agents, insecticides, antiprotozoal agents, and herbicides [3–5]. In addition, morpholine derivatives possess anti-inflammatory, antimicrobial and central nervous system activities [6]. The morpholine nucleus incorporated in a wide variety of therapeutically important drugs like linezolid, which belongs to the oxazolidinone class of anti-infectives and is used for the treatment of infections caused by Gram-positive bacteria [7]. On the other hand, the complexation capacity of thiourea derivatives and the biological activities of thiourea complexes are well recognized for different biological systems [8–10].

Among the transition metal, cobalt, nickel, and silver ions have been attracted the biologists attention due to their individual characteristics. A large number of reports on the antibacterial characteristics of cobalt complexes have developed in the literature and selecting Co complexes as the main subjects for the study in order to find effective antibacterial agents still being continued [8, 11]. Nickel is an essential trace element for bacteria, plants, animals, and humans [12]. There is spectroscopic evidence for nickel–methyl complexes in CODH of anaerobic bacteria [13]. For instance, the nickel transport system in *E. coli* composed of five proteins, *NiKABCDE*.

On the other hand, silver deposition has been found in the skin, the lungs, the gingiva, mucous membranes, and gastrointestinal tract [14, 15]. Essentially complex structures of silver-protein are take in within the body but have no physiological or biochemical roles [14, 16, 17]. Ag complexes have a very broad range of antibacterial activity and annihilate both Gram-positive and Gram-negative bacteria. Silver is a more lethal element to microorganisms than many other metals [18–20]. Actually, silver destructs the structure of

Supplementary information The online version of this article (https://doi.org/10.1038/s41429-019-0147-2) contains supplementary material, which is available to authorized users.

✉ Ali Reza Rezvani
ali@hamoon.usb.ac.ir

[1] Department of Chemistry, University of Sistan and Baluchestan, Zahedan P.O. Box 98135-674, Iran

[2] Institute of Physics, Academy of Sciences of the Czech Republic, Na Slovance 2, 182 21, Praha 8, Czech Republic

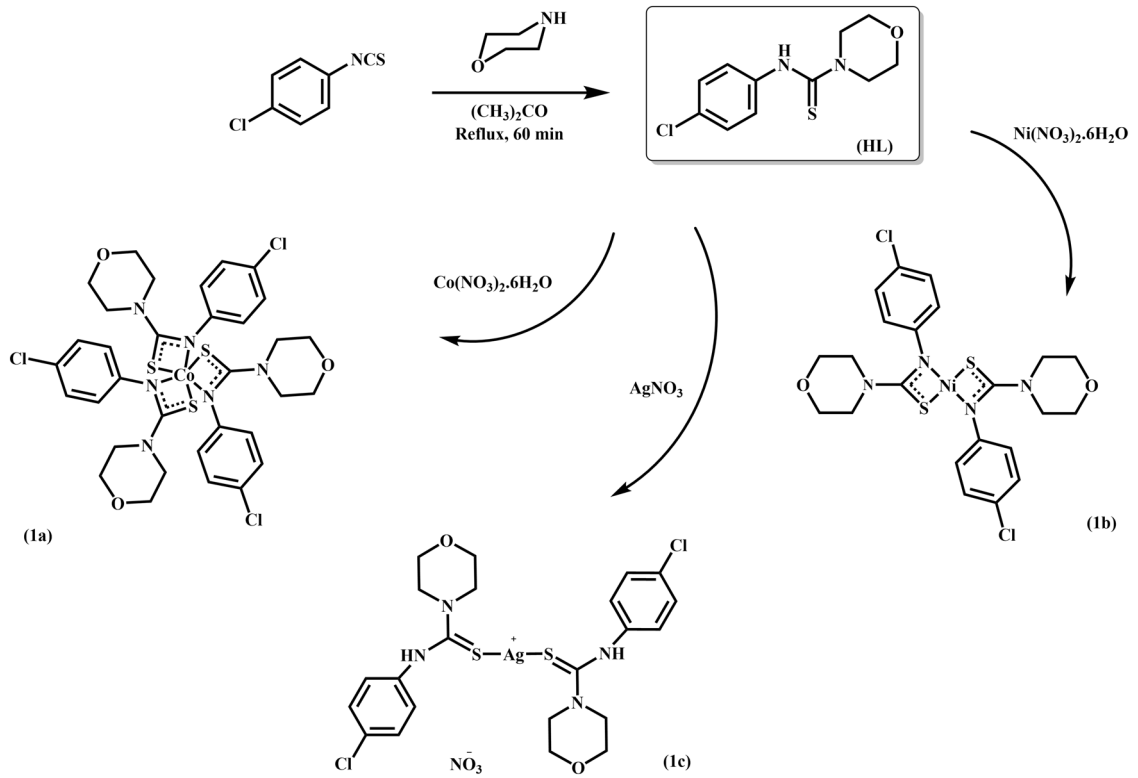

Scheme 1 .Synthetic route to **HL** ligand, **1a**, **1b**, and **1c** complexes

bacterial cell membrane, prevent the cell respiration, and increase or diminish the expression abundance of some enzymes [20]. Indeed, the mechanism for the antibacterial activity of silver complex is not correctly recognized; although it is accepted that they intervene with cell growth via interruption of cell metabolism, restraint of transport actions in the cell wall, and interaction with DNA [14].

In this research, we report the synthesis of a novel thiourea derivative, *N*-(4-chlorophenyl)morpholine-4-carbothioamide (**HL**) and its Co(III), Ni(II), and Ag(I) complexes (**1a**, **1b**, and **1c**) and their characterization by FT-IR, ^{1}H NMR, and UV-vis spectroscopy. For **HL** and its **1c** complex, crystal structures were determined using X-ray single-crystal diffraction methods. We also evaluated the antibacterial activities of these compounds using three methods, macro dilution (MIC), colony count and well diffusion. The relationship between the structures of these specimens and their antimicrobial activity was prospected based on density functional theory (DFT) calculations.

Results and discussion

Synthesis

The reaction between 4-chlorophenyl isothiocyanate and morpholine in acetone resulted in the **HL** ligand (Scheme 1). This ligand was recrystallized by ether diffusion into the *N*,*N*-Dimethylformamide solution of the ligand.

According to the Scheme 1, the Co(III), Ni(II), and Ag(I) complexes, **1a**, **1b**, and **1c** were prepared by adding a hot methanolic solution (50 °C) of the respective metal nitrate to a solution of the **HL** ligand in the molar ratio of 1:3 for **1a** and 1:2 for **1b** and **1c**. The synthesized Co(III), Ni(II), and Ag(I) complexes are soluble in $CHCl_3$, DMF, and DMSO. These compounds were characterized by UV-vis, ^{1}H NMR, FT-IR spectroscopy and the single-crystal X-ray diffraction analysis.

FT-IR spectral studies

In the FT-IR spectra of **HL** ligand, the band at 3159 cm^{-1} could be attributed to the stretching frequencies of the N–H group. Stretching vibrations of C = S bond was observed at 1323 cm^{-1}. Symmetric and asymmetric stretching vibrations of (-CH_2) protons appeared at 2861–2908 cm^{-1}. The absence of ν(S-H) band at about 2570 cm^{-1} and the presence of the ν(N-H) band at about 3159 cm^{-1} indicated formation of the thione tautomer in the solid state (Figure S1a in the supplementary content). After complexation of the **HL** ligand to the Co(III) and Ni(II) the N-H stretching vibrations disappeared due to the loss of the H bonded to the N atom of thioamide group (Figure S1b and c, in the

supplementary content). Also, the vibrational frequencies corresponding to C = S group in the free ligand were shifted towards down fields upon the complexation, confirming that the **HL** ligand is coordinated to the cobalt and nickel ions via the nitrogen and sulfur atoms in a form of neutral complexes (**1a** and **1b**) [21, 22].

The FT-IR spectrum of the **1c** complex demonstrates bands similar to those of ligand with a slight shift to the lower/upper wavenumbers owing to its coordination with Ag(I) metal center in the complex. For example, the characteristic band at 3208 and 1304 cm^{-1} can be assigned to N-H and C-S stretching vibration of **1c** complex. Therefore, the presence of the ν(N-H) band and shifting of the ν(C-S) band towards lower wavenumber confirmed that the **HL** coordinates to the Ag(I) via S atom, unlike Co(III) and Ni (II) complexes. The infrared absorption band of the nitrate anion in this complex exhibits that the nitrate isn't coordinated to Ag(I) center. This fact was deduced from the strong new band revealed at 1343 cm^{-1} (Figure S1d in the supplementary content) [14, 23].

NMR spectral studies

The ^{1}H NMR spectra were recorded at room temperature at 300 MHz in DMSO-d_6 for ligand, Co(III) and Ag(I) complexes and in $CDCl_3$ for Ni(II) complex (Figure S2 a-d, in the supplementary content). The formed thione tautomer of **HL** instead of thiol tautomer was proved by presence of NH resonances at δ 9.42 ppm and absence of SH resonances. The phenyl protons and the diastereotopic hydrogens of -CH_2 (morpholine moiety) were observed at δ 7.32–7.39 and δ 3.65–3.92 ppm, respectively.

Based on the results, complexation of **HL** to Ag(I) through S atom is approved by the presence of the N–H signal at δ 10.01 ppm. Indeed, pursuant to the Lewis acids and bases theory, the soft Ag(I) metal center tends to coordinate to the sulfur atom of the ligand than the nitrogen or oxygen atoms. In the spectrum of **1c**, each peak is shifted toward upfield from its normal peak position corresponding to **HL**. The diastereotopic hydrogens of -CH_2 (morpholine moiety) and phenyl protons are observed at δ 3.72–3.75, δ 3.91–3.94 and δ 7.19–7.46 ppm, respectively.

On the other hand, the loss of NH resonances in the **1a** and **1b** metal complexes confirmed that the chelation of **HL** ligand to the Co(III) and Ni(II) occurs via N and S atoms. The diastereotopic hydrogens of -CH_2 morpholine moiety appeared at δ 3.06–3.78 and δ 3.14–3.86 ppm for **1a** and **1b**, respectively. Similarly, the characteristic signal of the phenyl protons corresponding to **1a** and **1b** was observed at δ 6.40–7.64 and δ 6.55–7.26 ppm, respectively. Both FT-IR and NMR data are in agreement with the proposed structures [24].

Electronic absorption spectroscopy

$CHCl_3$ solutions of the thiourea ligand **HL** and its metal complexes **1a**, **1b**, and **1c** were prepared and their electronic absorption spectra were recorded in the range of 200–800 nm. For **HL**, the observed absorption bands at 240 and 270 nm were assigned to intra-ligand charge transfer transitions π–π^* (phenyl ring) and n–π^* corresponding to C = S bond [25, 26].

As expected from the results of FT-IR spectroscopy, no significant shifts in the π–π^* transitions were observed after complexation but a bathochromic shift that corresponding to the n–π^* transitions of C-S bond were recognized, which demonstrated that the ligand coordinated to the Co(III) and Ni(II) through the N and S atoms. Accordingly, in the **1a** and **1b**, bands above 340 nm are attributed to charge transfer processes, probably from the ligand to the metal. Absorption bands at higher wavelengths in the visible region (650 and 635 nm for **1a** and **1b**, respectively) were due to d–d transitions. In the **1c** complex, the absorption band corresponding to the n–π* transition of C = S is demonstrating a bathochromic shift (265 nm) due to the complexation of thione sulfur atoms to metal ion. Generally, in electronic absorption spectra of **1c** complex, no d–d transition was observed due to d^{10} electronic configuration of Ag(I) ion [27–29].

Description of crystal structures

Crystal structure of HL

The structure of **HL** was affirmed by the results of single-crystal X-ray structure determination. The molecule of this compound is shown in Fig. 1, details about crystal data collection and structure refinement and important bond lengths and angles are summarized in Table 1. The bond length of thiocarbonyl (C7-S1 = 1.685(5) Å) lies between values of a single and a double bond [30, 31]. On the other hand, due to the delocalization of electron density in the ligand, the mentioned C–N bonds, C7-N1 = 1.365(1) Å,

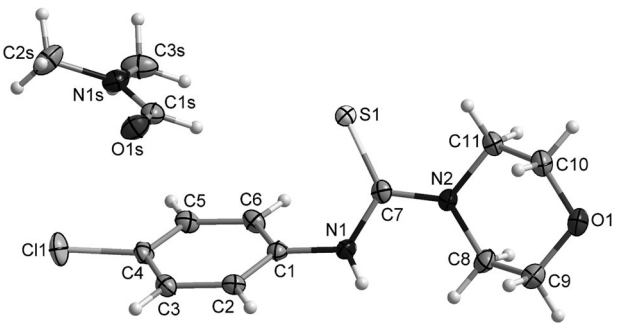

Fig. 1 ORTEP diagram of **HL** ligand. CCDC number is 1884234

Table 1 Summary of X-ray diffraction data and selected bond lengths (Å), angles (°), torsion angles (°) for **HL** ligand and Ag(I) complex (**1c**)

Compound	HL	1c	Bond lengths (Å) of HL		Bond lengths (Å) of 1c	
Empirical formula	$C_{14}H_{20}Cl_1N_3O_2S_1$	$C_{22}H_{26}Ag_1Cl_2N_5O_{5.335}S_2$	C7-S1	1.6855(10)	Ag1-S1b	2.3969(6)
Formula weight	329.8	688.7	C7-N1	1.3652(17)	S1b-C1b	1.717(2)
Wavelength (Å)	0.71073	1.54184	C1-N1	1.4178(15)	C1b-N2b	1.350(2)
Crystal system	Triclinic	Triclinic	N1-H1n1	0.880(4)	C1b-N1b	1.343(3)
Space group	P $\bar{1}$	P $\bar{1}$	C7-N2	1.3523(15)	N2b-H1n2b	0.86(2)
a (Å)	8.7614(3)	10.7920(2)	C11-N2	1.4708(17)	C6b-N2b	1.416(3)
b (Å)	9.8877(4)	10.8255(2)	C8-N2	1.4669(14)	Ag1-S1a	2.3925(5)
c (Å)	10.3554(4)	13.2124(2)	C9-O1	1.4217(18)	S1a-C1a	1.7197(2)
α (°)	73.963(4)	66.1841(17)	C4-Cl1	1.7458(12)	C1a-N1a	1.338(2)
β (°)	84.073(3)	74.4009(14)	C1s-O1s	1.234(2)	C1a-N2a	1.353(2)
γ (°)	66.620(3)	75.0505(15)	N1s-C1s	1.3265(15)	N2a-H1n2a	0.86(1)
V (Å^3)	791.37(6)	1340.45(4)	N1s-C2s	1.4537(19)	C6a-N2a	1.416(2)
Z	2	2	N1s-C3s	1.455(2)		
D_{calc} (g/cm^3)	1.3842	1.7064			Bond angles (°) of **1c**	
μ (Mo $K\alpha$)	0.381	9.685			S1a-Ag1-S1b	175.007(2)
F(000)	348	697	Bond angles (°) of **HL**		N1b-C1b-N2b	117.09(19)
θ range (°)	3.47 to 29.64	3.72 to 74.47	S1-C7-N1	122.73(8)	S1b-C1b-N2b	123.67(17)
Reflection collected	13152	22315	S1-C7-N2	122.35(10)	C1b-N2b-H1n2b	119.3(15)
Independent reflection	3957	5407	N1-C7-N2	114.88(9)	N1a-C1a-N2a	115.97(16)
R_{int}	0.0207	0.0284	C7-N1-C1	123.16(9)	S1a-C1a-N2a	124.08(14)
Data/parameters	3957/193	5407/367	C7-N2-C11	122.34(9)	S1a-C1a-N1a	119.95(12)
GOF on F^2	1.40[a]	1.35[a]			C1a-N2a-H1n2a	114.9(14)
R_1 [$I > 3\sigma(I)$]	0.0296	0.0223	Torsion angles (°) of **HL**			
wR_2 [$I > 3\sigma(I)$]	0.0843	0.0689	S1-C7-N2-C11	4.6(2)	Torsion angles (°) of **1c**	
R_1 (all data)	0.0381	0.0229	S1-C7-N2-C8	−163.52(12)	Ag1-S1a-C1a-N1a	−25.976(164)
wR_2 (all data)	0.0905	0.0697	S1-C7-N1-C1	8.6(2)	Ag1-S1b-C1b-N1b	21.522(178)
Largest diff. peak/hole (e Å^{-3})	0.22/−0.16	0.45/−0.42	C1-N1-C7-N2	−173.61(13)		

[a]JANA2006 does not refine the weighting scheme. Therefore, the goodness of fit is usually fairly above 1, especially for well-exposed data bearing information about bonding electrons.

C7-N2 = 1.353(3) Å, become shorter in comparison with the typical single C–N bond length of 1.479 Å [C8-N2 = 1.466(9) Å and C11-N2 = 1.470(8) Å] [32, 33]. This delocalization is also confirmed by values of the angles N1-C7-N2 = 114.87(7)°, N1-C7-S1 = 122.73(6)° and N2–C7-S1 = 122.35(0)° indicating sp^2 hybridization on the C7 atom [34].

Crystal structure of 1c

Figure 2 shows that the Ag center is coordinated to two ligands in a neutral monodentate (S) binding mode, giving rise to a nearly linear geometry around Ag [S1a-Ag1-S1b = 175.007(19)°]. The crystal structure also contains a free disordered NO_3 anion and two partially occupied crystal water molecules, one of them being weakly coordinated to Ag (Ag1-O2w = 2.5115(216) Å). A summary of selected bond lengths and bond angles for the **1c** complex is given in

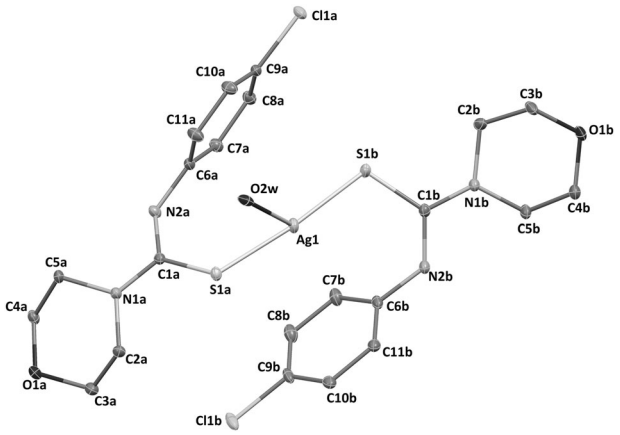

Fig. 2 ORTEP diagram of **1c** complex. CCDC number is 1884216. (The hydrogens of water molecules and nitrate ion were omitted for more clarity)

Table 1. The C–S bond lengths for **1c** are longer than that for **HL** [35, 36]. Other bond lengths and angles are in good agreement. For other newly synthesized complexes (**1a** and **1b**) several attempts failed to obtain a single-crystal suitable for X-ray crystallography.

Antibacterial activities

The bactericidal properties of **HL**, **1a**, **1b**, **1c**, and the reference antibiotics amikacin (AMK-30 µg) and gentamicin (GEN-10 µg) were examined against two Gram-negative; *Escherichia coli* (ATCC 25922) and *Pseudomonas aeruginosa* (ATCC 27853) and two Gram-positive; *Staphylococcus aureus* (ATCC 25923) and *Enterococcus faecalis* (ATCC11700) bacteria. DMSO was employed as a negative control while amikacin and gentamicin were utilized as positive controls for Gram-positive and Gram-negative antibacterial activity, respectively. Silver sulfadiazine (AgSD) is regarded as reference Ag(I) specimen for susceptibility testing [14, 37]. Macro dilution, colony count, and well diffusion methods were employed to characterize the antimicrobial activity of these reagents.

Minimum inhibitory concentration (MIC) assay

In our investigation, the metal salts all presented moderate MIC values against the studied bacteria strains (MIC values below 0.1 mg/mL are considered significant, between 0.1 and 0.5 mg/mL moderate, between 0.5 and 1.0 mg/mL weak, and above 1.0 mg/mL negligible) [38–40]. On the other hand, although **HL** ligand also showed a moderate MIC value against *E. coli*, *P. aeruginosa*, and *S. aureus*, its activity against *E. faecalis* was weak. As for the metal complexes, a significant increase of the bactericidal activity was observed in comparison to the free ligand. The order by antimicrobial activity was **1c > 1b > 1a > HL**. The enhanced activity of these complexes in comparison with the free ligand can be explained by the Ovetone's concept explaining the relationship between the bactericidal activity and lipophilicity. As we know, the lipid membrane that envelopes the cell favors the passage of lipid-soluble substances [41–47]. Furthermore, the presence of the chlorine moiety in the structure of these reagents may also contribute to their antibacterial effect due to the hypochlorous acid formation. This acid crumbles forming hydrochloric acid and oxygen, and the oxygen damages microorganisms through oxidizing cellular parts. Chlorine compounds can also interact and combine with proteins and enzymes of membranes and as a result, destroy the microbes or prevent their growth by obstruction of their active sites [48]. Meanwhile, the presence of the chlorine atom and the morpholine group increases the lipophilicity and the electron-withdrawing effect on these samples, and this can also improve the bactericidal effects [49, 50]. Although antimicrobial activity of all complexes was observed to have the notable effect versus all tested Gram-negative and Gram-positive bacteria, they exhibited lower activity compared to standard antibiotics amikacin and gentamicin.

Well diffusion assay

The results of well-diffusion method for antimicrobial activity of synthesized samples show the highest zone of inhibition (19.7 mm) for **1c** against *E. coli*. The results (Table 2) show the studied compounds possess antibacterial activity against the above-mentioned Gram-negative and Gram-positive bacteria, and the activity against the Gram-negative bacteria is larger. The efficacy of these compounds is controlled by the cell-wall thickness and the polarity of the inner cell membrane, so the permeation into the bacterial strains of some agents can be facilitated [51–56]. Gram-negative bacterium has a thin peptidoglycan layer that an outer protein-phospholipid-lipopolysaccharide membrane covers that, whereas a Gram-positive bacterium has a thick peptidoglycan layer that contains teichoic and lipoteichoic acid. As a result, the cell wall of Gram-negative

Table 2 Results of minimal inhibitory concentrations (MIC, mg/mL) and zones of inhibition (ZI, diameter/mm) of all compounds against the studied bacterial strains

Samples	*E. coli* ATCC 25922		*P. aeruginosa* ATCC 27853		*S. aureus* ATCC 25923		*E. faecalis* ATCC 11700	
	MIC (mg/mL)	ZI (mm)	MIC (mg/mL)	ZI (mm)	MIC (mg/mL)	ZI (mm)	MIC (mg/mL)	ZI (mm)
HL	0.256	—	0.256	—	0.512	—	1.024	—
1a	0.016	14.3	0.032	13.3	0.032	13	0.064	13
1b	0.007	17.5	0.009	16	0.013	15.9	0.021	14
1c	0.001	19.7	0.001	19.5	0.002	19.5	0.004	18.7
DMSO	—	—	—	—	—	—	—	—
AgSD	0.022	—	0.028	—	0.022	—	0.023	—
Amikacin	—	—	—	—	0.0025	17.9	0.003	17.2
Gentamicin	0.001	20.2	0.0015	19.4	—	—	—	—

bacteria is more polar [57, 58]. As a result, the bactericidal properties of **HL** ligand and its complexes against *P. aeruginosa* and *E. coli* is higher than against *S. aureus* and *E. faecalis* [59]. On the other hand, for all tested bacterial strains, the antibacterial activity of complexes was higher than for the free ligand. Indeed, the coordination of metal ions to the ligand enhanced the antibacterial activities. This is maybe caused by a synergistic effect involving Co(III), Ni(II), and Ag(I) ions and the thiourea ligand.

Colony count assay

As shown in Fig. 3, the consequences achieved from the colony count assay corroborate the results of MIC as well as of well diffusion. The **1c** complex demonstrates stronger activity than the other specimens and inhibits all bacteria strains, *E. coli*, and *S. aureus*, in the lowest time.

Overall, the **1c** complex has more ability than the other reagents to penetrate the cell wall or the lipid layer of the cell membrane. This is caused by relative lability of this complex compared with the Co and Ni complexes, Therefore, **1c** interacts more adequately with biological ingredients inside the cytoplasm, interlinks to bacterial surface and as a result, frustrates the microorganism activities by either changing the cell wall or the membrane function or barricade replication [60]. On the other hand, the lower activity of the **1a**, and **1b** complexes can be attributed to low lipid solubility. Therefore, the metal ion cannot reach the desired site of action of the cell wall [61, 62].

Structure-activity relationship

The molecular structures of **HL**, **1a**, **1b**, and **1c** compounds were optimized by using the DFT method (B3LYP) at

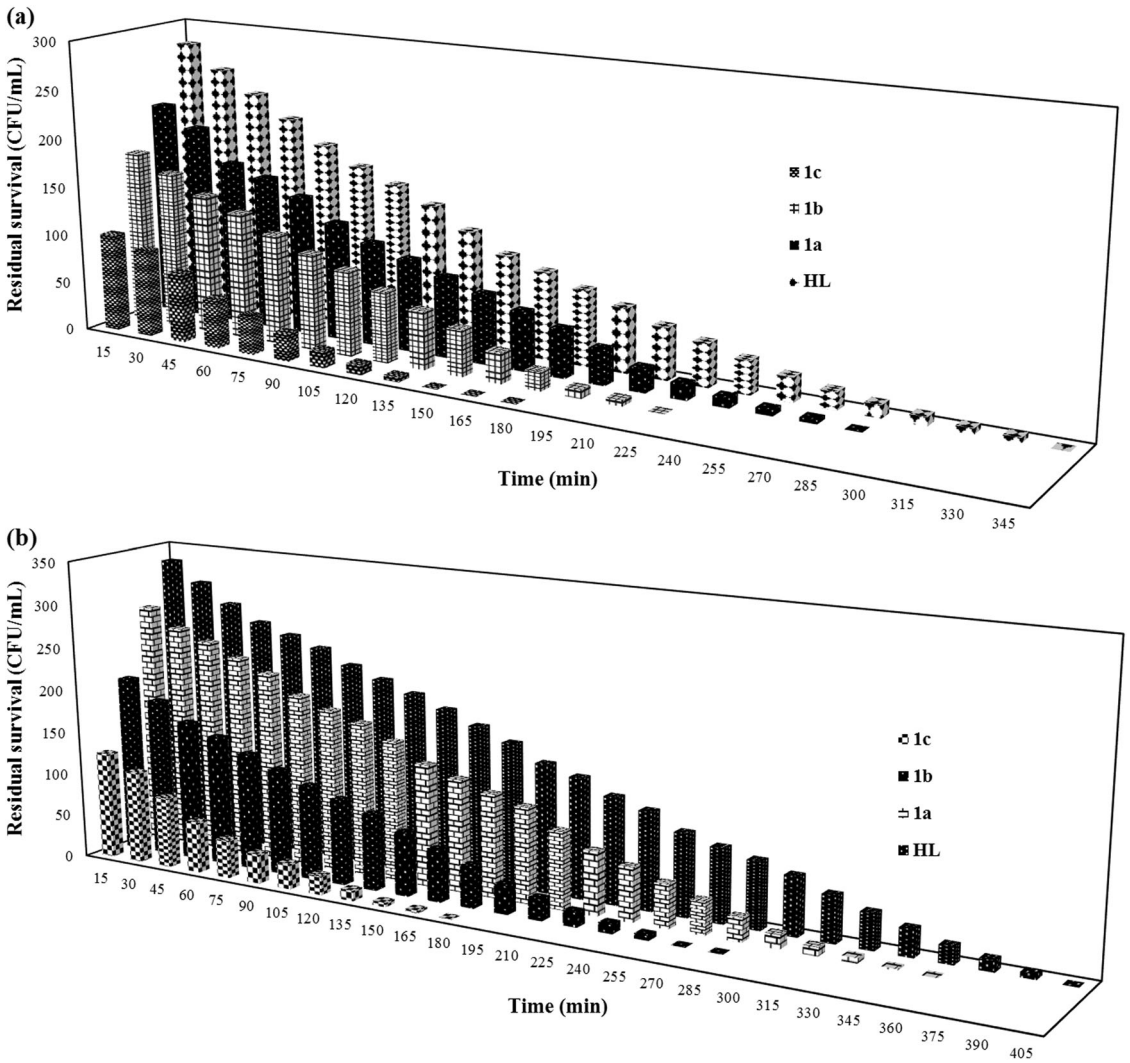

Fig. 3 Plot of the survival number of **a** *E. coli* ATCC 25922 and **b** *S. aureus* ATCC 25923 with **HL** ligand, **1a**, **1b**, and **1c** complexes in colony count method

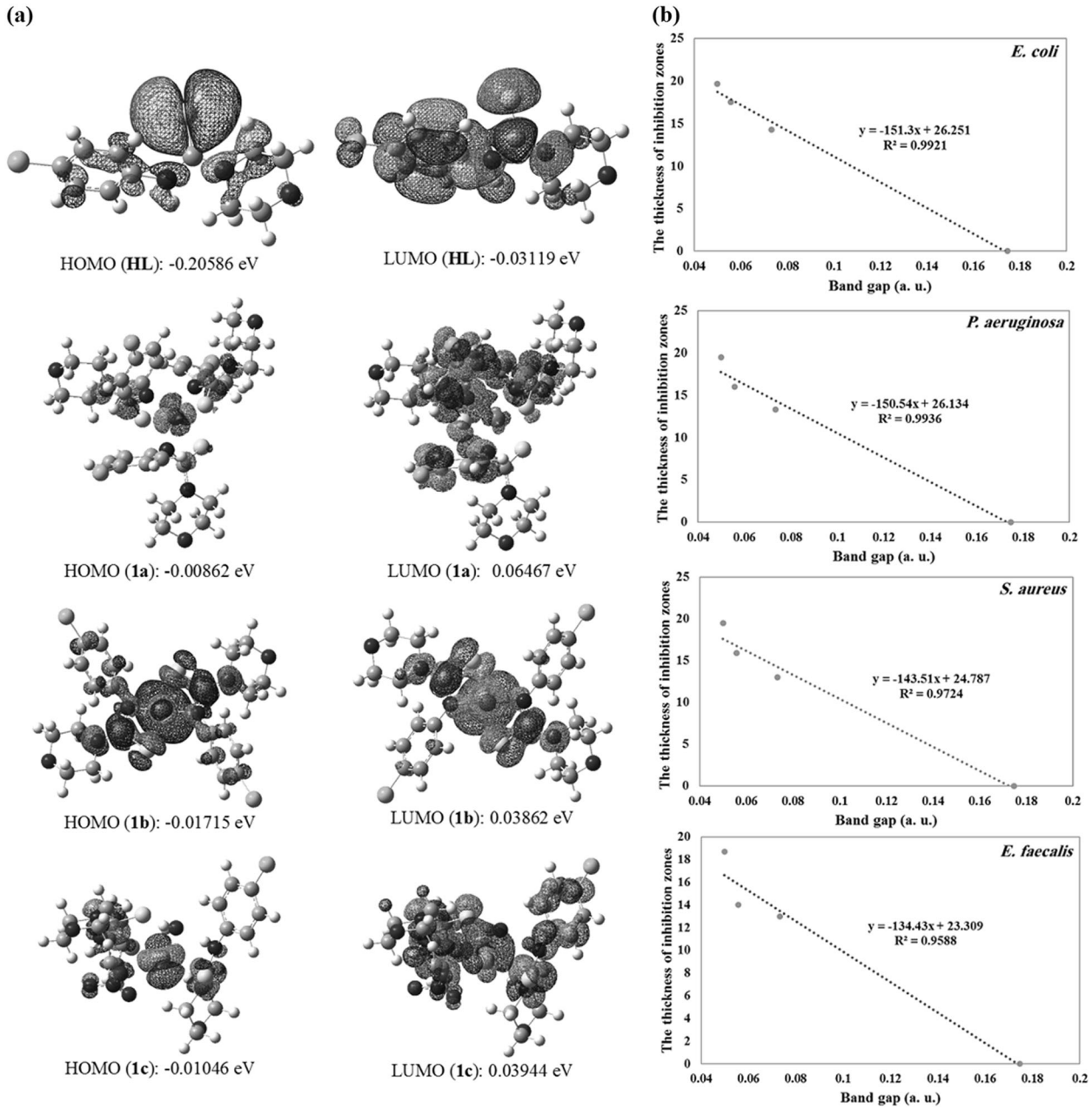

Fig. 4 **a** Frontier molecular orbitals of the studied specimens; **b** The linear relations of the differences between the band gap and the zone of inhibitions for the studied bacteria strains in **HL**, **1a**, **1b**, and **1c**

6-31 G* and LANL2DZ basis set level. After that, DFT results were obtained for the frontier molecular orbital energies. Fig. 4(a) demonstrates the frontier molecular orbitals (FMOs) of these samples.

FMOs have a substantial role in the advent of optical and electrical properties. The band gap is also associated with antimicrobial properties. The narrower band gap facilitates the electron transfer from the electron-donor groups to the electron-acceptor groups, that can cause interruption of the cellular respiration process, deactivation of several cellular enzymes and denaturation of one or more cellular proteins and ultimately lead to cell death [63, 64].

The inverse relationship between the size of the band gap (ΔE_{L-H}) and the bactericidal activities of these samples were approved by these conclusions. i.e., if the difference between HOMO and LUMO energies is smaller, the greatness of the antibacterial activity gets more [31].

Also, the linear relationship between the thickness of zone of inhibitions for above-named standard bacterial strains and band gap values can be found by an accurate

examination of the computational conclusions. Pursuant to Fig. 4(b), the **1c** complex has the narrowest band gap, which corresponds to its strongest bactericidal activity among the investigated samples [8].

Conclusion

In the present research, we synthetized a novel thiourea ligand and its Co(III), Ni(II) and Ag(I) complexes. Their structures were characterized by FTIR, UV-vis, ^{1}H NMR. For **HL** and **1c**, we also performed single-crystal X-ray diffraction analysis. These characterizations proposed the **HL** coordinated to the Co(III), Ni(II) ions through N and S atoms and constructed a four-membered chelate rings, while to Ag(I) it coordinated via S atom as a monodentate ligand. For all of the samples, antimicrobial activity was examined against Gram-negative (*E. coli* and *P. aeruginosa*) and Gram-positive (*S. aureus* and *E. faecalis*) bacteria by three methods, showing that they have good bactericidal activity in the order of **1c > 1b > 1a > HL**. While the **HL** ligand did not demonstrate a remarkable antibacterial activity, its related complexes, especially **1c**, had the best performance versus all tested strains.

Materials and methods

Experimental instruments

Infrared spectra were recorded on KBr pellets using a PerkinElmer 781 spectrophotometer FTIR. ^{1}H NMR was recorded in DMSO-d_6 and $CDCl_3$ solvents on a BRUKER 300 MHz AVANCE III spectrometer with tetramethylsilane as internal reference. The melting points were measured on an Electro-thermal 9100 apparatus. Single-crystal X-ray data were collected on Gemini diffractometer of Rigaku Oxford Diffraction using the graphite monochromated MoKα radiation from a sealed X-ray tube and CCD detector Atlas S2 at 120 K. For structure plots, Diamond 4.5.2 was used.

All solvents and chemical materials were reagent grade and were purchased from Merck and Fluka, including 4-chlorophenyl isothiocyanate, $Co(NO_3)_2.6H_2O$, $Ni(NO_3)_2.6H_2O$, $AgNO_3$, morpholine, methanol, and acetone.

Preparation of the *N*-(4-chlorophenyl)morpholine-4-carbothioamide (HL)

The thiourea ligand was synthesized by dissolving 0.01 mol 4-chlorophenyl isothiocyanate and 0.01 mol morpholine in acetone. This mixture was refluxed for 1 h. After that, this solution was poured into 250 mL distilled water, resulting a white precipitate that was filtered off and washed with distilled water. The colorless crystals were obtained by ether diffusion into the DMF solution of ligand. Yield (87%). Mp: 158–160 °C. Selected FT-IR data (ν, cm^{-1}): 3159 (N-H), 2953–3097 (Ph-H), 2861–2908 (C-H), 1324 (C = S). ^{1}H NMR (DMSO-d_6; δ, ppm): 9.42 (s, 1 H, N-H), 7.31–7.41 (m, 4 H, Ph), 3.89–3.92 (t, 4 H, O-CH_2), 3.65–3.69 (t, 4 H, N-CH_2).

Preparation of Co complex (1a)

The desired complex was prepared by addition of the methanolic solution of $Co(NO_3)_2.6H_2O$ in 50 °C to the solution of **HL** ligand in 1:3 molar ratio and the resulting mixture was refluxed for 3 h. The dark green precipitates of the complex were filtered off and dried in vacuo. Yield (78%). Mp: 138–140 °C. Selected FT-IR data (ν, cm^{-1}): 2918–2965 (Ph-H), 2848 (C-H), 1233 (C = S). ^{1}H NMR (DMSO-d_6; δ, ppm): 6.40–7.46 (m, 12 H, Ph), 3.06–3.78 (m, 24 H, -CH_2).

Preparation of Ni complex (1b)

A similar procedure was carried out using **HL** (2 mmol) and $Ni(NO_3)_2.6H_2O$ (1 mmol) and refluxed for 3 h. The green precipitates were filtered off and dried in vacuo. Yield (75%). Mp: 280–282 °C. Selected FT-IR data (ν, cm^{-1}): 2919–3026 (Ph-H), 2848–2892 (C-H), 1241 (C = S). ^{1}H NMR ($CDCl_3$; δ, ppm): 6.55–7.26 (m, 8 H, Ph), 3.14–3.86 (m, 16 H, -CH_2).

Preparation of Ag complex (1c)

In a similar procedure, the Ag complex was obtained by the reaction of $AgNO_3$ with the ligand (molar ratio of 1:2) in methanol. The gray precipitates of the complex were filtered off and dried in vacuo. Yield (88%). Mp: 170–172 °C. Selected FT-IR data (ν, cm^{-1}): 3208 (N-H), 3044–3165 (Ph-H), 2858–2968 (C-H), 1343 (NO_3^-), 1304 (C = S). ^{1}H NMR (DMSO-d_6; δ, ppm): 10.01 (s, 2 H, N-H), 7.19–7.46 (m, 8 H, Ph), 3.91–3.94 (t, 8 H, -CH_2), 3.72–3.75 (t, 8 H, -CH_2).

X-ray crystallographic analysis

The measurement of **HL** was performed at 120 K on a Gemini diffractometer of Rigaku Oxford Diffraction using the graphite monochromated MoKα radiation from a sealed X-ray tube, and CCD detector Atlas S2. The measurement of **1c** was performed at 95 K on a SuperNova diffractometer of Rigaku Oxford Diffraction using the mirror-collimated CuKα radiation from a micro-focus sealed X-ray tube, and CCD detector Atlas S2. CrysAlis PRO software was utilized

for correction of reduction and absorption data [65]. The structures were solved using charge flipping methods and refined using Jana2006 [66, 67]. The residual electron density maps were plotted using MCE [68]. All hydrogen atoms could have been distinguished in difference Fourier maps and could have been refined to a reasonable geometry. According to common practice, H atoms bonded to C were kept in ideal positions with C–H 0.96 Å while positions of H atom bonded to N were refined with restrained bond lengths. In both cases, U_{iso}(H) was set to 1.2U_{eq}(C,N). All non-hydrogen atoms were refined using harmonic refinement.

Hydrogen atoms of partially occupied crystal water molecules (0.270(10) for O1w and 0.064(6) for O2w] in **1c** could not be determined because they were not present in a difference Fourier map. Moreover, **1c** contained a disordered NO_3 anion with two close positions occupied 0.774 (12) and 0.226(12). These positions were refined using the rigid body approach of Jana2006, and their occupancies were restricted to keep the full total occupancy.

In vitro antibacterial studies

The in vitro antimicrobial tests were examined against *P. aeruginosa*, ATCC 27853, and *E. coli*, ATCC 25922 (Gram-negative) and *S. aureus*, ATCC 25923, and *E. faecalis*, ATCC 11700 (Gram-positive) bacteria. Nutrient broth (NB) medium for both macro dilution (MIC) and colony count methods and Nutrient agar (NA) medium was used for the well-diffusion method. The bacterial strains were retained on agar slant at 4 °C and were sub-cultured on the fresh appropriate agar plate in incubators for 18–24 h prior to any antimicrobial analysis. To promote the solubility of these samples in water, they were dissolved in 10% DMSO solution. The same solution (without reagents) was used as negative control. The amikacin and gentamicin were used as positive control for Gram-positive and Gram-negative bacteria, respectively. Comparative investigation of the bactericidal activities of these samples was determined by using three following methods:

Macro-dilution (tube) broth method

According to the literature, 1 mL of Mueller-Hinton broth was added to the desired quantity of sample tubes (10 sample tubes) [69]. Then 1 mL stock solution of any compounds (**HL**, **1a**, **1b**, and **1c**) dissolved in 10% DMSO solution and added to the first test tubes. After that, different concentration of the ligand and its complexes (93.68, 46.83, 23.42,11.71, 5.85, 2.93, 1.46 µM) were prepared from initial solutions. 1 mL of the suspension of bacteria that had been adjusted to 0.5 McFarland in sterile peptone water, was added to each sample tubes. After mixing, the sample tubes were incubated at 37 °C for 24 h. Then, 100 µL samples were taken from each tube and were applied on the specified amount of the Nutrient Agar and incubated at 37 °C for 24 h. The lowest concentration of test compounds eliminating bacterial growth indicates the MIC (Minimum Inhibitory Concentration).

Colony count method

The bacteria strains have been streaked in nutrient broth medium (NB) contained **HL** ligand, **1a**, **1b**, and **1c** complexes suspension at the concentration of 20 µg/mL for measuring the rate of bacteria growth. These samples were appended into 10 mL NB medium which was added 200 µL bacteria at the concentration of 1.5×10^5 CFU. The same condition was used for preparing the blank samples by growth of the culture on the ligand and metal complexes free medium. Then a shaker platform was used to wiggle these samples at a speed of 200 rpm. After that, 100 µL of each bacteria suspension was dispersed on the Nutrient Agar medium. Finally, after 24 h of incubation at 37 °C the number of colonies forming units (CFUs) was counted by considering the dilution factor [33].

Agar well diffusion test

In vitro antimicrobial activity of all synthesized **HL** ligand and its Co(III), Ni(II), and Ag(I) complexes was investigated in an agar diffusion test. In a common method, the test bacteria were counted by dilution plate method. The cultured bacteria were spread on the agar medium by an appropriate sterile swab. After drying the plates, a well was created on the agar medium by sterilized cork borer. DMSO stock solutions of all compounds were diluted with sterile water to the test concentration of 100 µg/mL, were added (100 µL) to these wells by using a micropipette and then were incubated with different test bacteria. During this step, the growth of the inoculated bacteria was impressed by diffusion of the test solution. Subsequently, antimicrobial activity was assessed by measuring the diameter of the inhibition zones around the hole. The size of inhibition zones was determined visually. If the inhibition zone was greater than 6 mm the compounds were regarded as active [70–72].

Acknowledgements We thank the University of Sistan and Baluchestan for the financial support. The crystallographic part was supported by the project 18–10504 S of the Czech Science Foundation using instruments of the ASTRA lab established within the Operation program Prague Competitiveness—project CZ.2.16/3.1.00/24510.

Compliance with ethical standards

Conflict of interest The authors declare that they have no conflict of interest.

References

1. Veale EB, Tocci GM, Pfeffer FM, Krugerac PE, Gunnlaugsson T. Demonstration of bidirectional photoinduced electron transfer (PET) sensing in 4-amino-1,8-naphthalimide based thiourea anion sensors. Org Biomol Chem. 2009;7:3447–54.
2. Gopiraman M, Selvakumaran N, Kesavan D, Kim IS, Karvembu R. Chemical and physical interactions of 1-Benzoyl-3,3-disubstituted thiourea derivatives on mild steel surface: corrosion inhibition in acidic media. Ind Eng Chem Res. 2012;51:7910–22.
3. Pintér G, et al. Synthesis and antimicrobial activity of ciprofloxacin and norfloxacin permanently bonded to polyethylene glycol by a thiourea linker. J Antibiot. 2009;62:113–16.
4. Zhang YM, Pang HX, Cao C, Wei TB. Synthesis, crystal structure and biological activity of a new complex bis(1,1-diethyl-3-(3-fluorobenzoyl)-thiourea)nickel(II). Indian J Chem Sect A. 2007;46A:1787–91.
5. Kumura K, et al. Synthesis and antibacterial activity of novel lincomycin derivatives. II. Exploring (7 S)−7-(5-aryl-1,3,4-thiadiazol-2-yl-thio)−7-deoxylincomycin derivatives. J Antibiot. 2017;70:655–63.
6. Dixit PP, et al. Synthesis of 1-[3-(4-benzotriazol-1/2-yl-3-fluorophenyl)-2-oxo-oxazolidin-5-ylmethyl]-3-substituted-thiourea derivatives as antituberculosis agents. Eur J Med Chem. 2006;41:423–28.
7. Bektaş H, Ceylan S, Demirbaş N, Alpay-Karaoğlu S, Sökmen BB. Antimicrobial and antiurease activities of newly synthesized morpholine derivatives containing an azole nucleus. Med Chem Res. 2013;22:3629–39.
8. Yang W, et al. Synthesis, structures and antibacterial activities of benzoylthiourea derivatives and their complexes with cobalt. J Inorg Biochem. 2012;116:97–105.
9. Saha S, Dhanasekaran D, Chandraleka S, Thajuddin N, Panneerselvam A. Synthesis, characterization and antimicrobial activity of cobalt metal complex against drug resistant bacterial and fungal pathogens. Adv. Biol Res. 2010;4:224–29.
10. Parekh HM, Pansuriya PB, Patel MN. Characterization and antifungal study of genuine oxovanadium(IV) mixed-ligand complexes with Schiff bases. Pol J Chem. 2005;79:1843–51.
11. Chang EL, Simmers C, Knight DA. Cobalt complexes as antiviral and antibacterial agents. Pharmaceuticals. 2010;3:1711–28.
12. Frausto da Silva JJR, Williams RJP. The biological chemistry of the elements: the inorganic chemistry of life. 2nd ed. Oxford: Oxford University Press; 2001.
13. Zaky RR, Ibrahim KM, Gabr IM. Bivalent transition metal complexes of o-hydroxyacetophenone [N-(3-hydroxy-2-naphthoyl)] hydrazone: Spectroscopic, antibacterial, antifungal activity and thermogravimetric studies. Spectrochim Acta A. 2011;81:28–34.
14. Movahedi E, Rezvani AR. New silver, (I) complex with diazafluorene based ligand: Synthesis, characterization, investigation of in vitro DNA binding and antimicrobial studies. J Mol Struct. 2017;1139:407–17.
15. Wan AT, Conyers RAJ, Coombs CJ, Masterton JP. Determination of silver in blood, urine, and tissues of volunteers and burn patients. Clin Chem. 1991;37:1683–87.
16. Lansdown ABG. Critical observations on the neurotoxicity of silver. Crit Rev Toxicol. 2007;37:237–50.
17. Ray R, et al. Anticancer and antimicrobial metallopharmaceutical agents based on palladium, gold, and silver *N*-heterocyclic carbene complexes. J Am Chem Soc. 2007;129:15042–53.
18. Fu-Ren F, Allen JF. Chemical, electrochemical, gravimetric, and microscopic studies on antimicrobial silver films. J Phys Chem B. 2002;106:279–87.
19. Monteiro DR, et al. The growing importance of materials that prevent microbial adhesion: antimicrobial effect of medical devices containing silver. Int J Antimicrob Agents. 2009;34:103–10.
20. Rizzotto M. Metal Complexes as Antimicrobial Agents. In: Bobbarala V, editor. A Search for Antibacterial Agents. 1st ed. Croatia: InTech Janeza Trdine, Rijeka; 2012. p. 73–88.
21. Malviya M, et al. Muscarinic receptor 1 agonist activity of novel *N*-arylthioureas substituted 3-morpholino arecoline derivatives in Alzheimer's presenile dementia models. Bioorg Med Chem. 2008;16:7095–101.
22. Nakamoto K, editor. Infrared and Raman Spectra of Inorganic and Coordination Compounds, Part B: Applications in Coordination, Organometallic, and Bioinorganic Chemistry. 6th ed. New Jersey: John Wiley & Sons, Inc.; 2009.
23. Shahabadi N, Kashanian S, Ahmadipour Z. DNA binding and gel electrophoresis studies of a new silver(I) complex containing 2,9-dimethyl-1,10-phenanthroline ligands. DNA Cell Biol. 2011;30:187–94.
24. Lever ABP, editor. Inorganic electronic spectroscopy. 2nd ed. Amsterdam, New York: Elsevier; 1984.
25. Atiş M, Karipcin F, Sarıboğa B, Taş M, Çelik H. Structural, antimicrobial and computational characterization of 1-benzoyl-3-(5-chloro-2-hydroxyphenyl)thiourea. Spectrochim Acta Part A. 2012;98:290–301.
26. Barret J, Deghaidy FS. Some new assign electron transit thiones. Spectrochim Acta Part A. 1975;31:707–13.
27. Knoblauch S, et al. Synthesis, crystal structure, spectroscopy, and theoretical investigations of tetrahedrally distorted copper(II) chelates with $[CuN_2S_2]$ coordination sphere. Eur. J. Inorg. Chem. 1999;1999:1393–403.
28. Klingele MH, Boyd PDW, Moubaraki B, Murray KS, Brooker S Probing the dinucleating behaviour of a bis-bidentate ligand: Synthesis and characterization of some di- and mononuclear cobalt(II), nickel(II), copper(II) and zinc(II) complexes of 3,5-di (2-pyridyl)-4-(1H-pyrrol-1-yl)-4H-1,2,4-triazole. Eur. J. Inorg. Chem. 2006;2006:573–89.
29. Binzet G, Arslan H, Flörke U, Külcü N, Duran N. Synthesis, characterization and antimicrobial activities of transition metal complexes of *N*,*N*-dialkyl-*N*′-(2-chlorobenzoyl)thiourea derivatives. J Coord Chem. 2006;59:1395–406.
30. Hernández W, et al. Synthesis, characterization and antitumor activity of *cis*-bis(acylthioureato) platinum(II) complexes, *cis*-$[PtL_2]$ [HL^1 = *N,N*-diphenyl-*N'*-benzoylthiourea or HL^2 = *N,N*-diphenyl-*N'*-(*p*-nitrobenzoyl)thiourea]. Bioinorg Chem Appl. 2003;1:271–84.
31. Rakhshani S, Rezvani AR, Dušek M, Eigner V. Design and synthesis of novel thiourea metal complexes with controllable antibacterial properties. Appl Organomet Chem. 2018; 32:4342–55. 32
32. Bourne S, Koch KR Intramolecular hydrogen-bond controlled unidentate co-ordination of potentially chelating *N*-acyl-*N*′-alkylthioureas: Crystal structure of *cis*-bis(*N*-benzoyl-*N*′-propylthiourea) dichloroplatinum(II). J. Chem. Soc., Dalton Trans. 1993;1993:2071–72.
33. Weast RC, editor. Handbook of chemistry and physics. 64th ed. Boca Raton, FL: CRC; 1983–1984.
34. Emen MF, Arslan H, Külcü N, Flörke U, Duran N. Synthesis, characterization and antimicrobial activities of some metal complexes with *N'*-(2-chlorobenzoyl)thiourea ligands: the crystal structure of *fac*-$[CoL_3]$ and *cis*-$[PdL_2]$. Pol J Chem. 2005;79:1615–26.
35. Nawaz S, Tahir MN, Nadeem MA, Mehmood B, Ahmad S. Crystal structure of bis(thiourea-κ*S*)bis(triphenylphosphane-κ*P*) silver(I) nitrate. Acta Crystallogr E. 2015;71:220–2.
36. Tahir MN, et al. Synthesis and characterization of silver(I) complexes of thioureas and thiocyanate: crystal structure of polymeric

(1,3-diazinane-2-thione) thiocyanato silver(I). Z. Naturforsch. B: Chem Sci. 2015;70:541–6.
37. Yilmaz VT, et al. Di- and polynuclear silver (I) saccharinate complexes of tertiary diphosphane ligands: synthesis, structures, in vitro DNA binding, and antibacterial and anticancer properties. J Biol Inorg Chem. 2014;19:29–44.
38. Tanaka JCA, da Silva CC, de Oliveira AJB, Nakamura CV, Dias Filho BP. Antibacterial activity of indole alkaloids from Aspidosperma ramiflorum. Braz J Med Biol Res. 2006;39:387–91.
39. Espírito Santo C, et al. Bacterial killing by dry metallic copper surfaces. Appl Environ Microbiol. 2011;77:794–802.
40. Ibrahim M, et al. Copper as an antibacterial agent for human pathogenic multidrug resistant *Burkholderia cepacia* complex bacteria. J Biosci Bioeng. 2011;112:570–76.
41. Urquiza NM, et al. Inhibition behavior on alkaline phosphatase activity, antibacterial and antioxidant activities of ternary methimazole-phenanthroline-copper(II) complex. Inorg Chim Acta. 2013;405:243–51.
42. Kalanithi M, Rajarajan M, Tharmaraj P. Synthesis, spectral, and biological studies of transition metal chelates of N-[1-(3-aminopropyl)imidazole]salicylaldimine. J Coord Chem. 2011; 64:842–50.
43. Sumathi S, Tharmaraj P, Sheela CD, Ebenezer R, Saravana Bhava P. Synthesis, characterization, NLO study, and antimicrobial activities of metal complexes derived from 3-(3-(2-hydroxyphenyl)-3-oxoprop-1-enyl)-4H-chromen-4-one and sulfanilamide. J Coord Chem. 2011;64:1673–82.
44. Sumathi S, Tharmaraj P, Sheela CD, Ebenezer R. Synthesis, spectral, bioactivity, and NLO properties of chalcone metal complexes. J Coord Chem. 2011;64:1707–17.
45. Chandraleka S, et al. Antimicrobial mechanism of copper (II) 1,10-phenanthroline and 2,2′-bipyridyl complex on bacterial and fungal pathogens. J Saudi Chem Soc. 2014;18:953–62.
46. Patel MN, Dosi PA, Bhatt BS, Thakkar VR. Synthesis, characterization, antibacterial activity, SOD mimic and interaction with DNA of drug based copper(II) complexes. Spectrochim Acta Part A. 2011;78:763–70.
47. Nirmala G, et al. Synthesis, characterization, crystal structure and antimicrobial activities of new *trans N,N*-substituted macrocyclic dioxocyclam and their copper(II) and nickel(II) complexes. Polyhedron . 2011;30:106–13.
48. Arias ME, Gomez JD, Cudmani NM, Vattuone MA, Isla MI. Antibacterial activity of ethanolic and aqueous extracts of *Acacia aroma* Gill. ex Hook et Arn. Life Sci. 2004;75:191–202.
49. Despaigne AAR, et al. Organotin(IV) complexes with 2-acetylpyridine benzoyl hydrazones: ntimicrobial activity. J Braz Chem Soc. 2010;21:1247–57.
50. Somashekhar M, Sonnad B, Tare B, Heralagi RV, Lokapure S. Synthesis and antimicrobial activity of 5[4(morpholin-4-yl) phenyl] 1,3,4 oxadiazole 2-yl sulphonyl acetohydrazide derivatives. Int J Med Pharm Res. 2014;2:462–71.
51. Khosravi F, Mansouri-Torshizi H. Antibacterial combination therapy using Co^{3+}, Cu^{2+}, Zn^{2+} and Pd^{2+} complexes: their calf thymus DNA binding studies. J Biomol Struct Dyn. 2017;35:1–20.
52. Amininezhad SM, Rezvani A, Amouheidari M, Amininejad SM, Rakhshani S. The antibacterial activity of SnO_2 nanoparticles against *Escherichia coli* and *Staphylococcus aureus*. Zahedan. J Res Med Sci. 2015;17:1053–58.
53. Talebian N, Amininezhad SM, Doudi M. Controllable synthesis of ZnO nanoparticles and their morphology-dependent antibacterial and optical properties. J Photochem Photobiol B. 2013;120:66–73.
54. Pal A, Pehkonen SO, Yu IE, Ray MB. Photocatalytic inactivation of Gram-positive and Gram-negative bacteria using fluorescent light. J Photochem Photobiol A. 2007;186:335–41.
55. Rincón AG, Pulgarin C. Bactericidal action of illuminated TiO_2 on pure *Escherichia coli* and natural bacterial consortia: post-irradiation events in the dark and assessment of the effective disinfection time. Appl Catal B. 2004;49:99–112.
56. Pal A, Pehkonen SO, Yu LE, Ray MB. Photocatalytic inactivation of Gram-positive and Gram-negative bacteria using fluorescent light. J Photochem Photobiol A: Chem. 2007;186:335–41.
57. Balyuzid HHM, Reaveleyr A, Burge E. X-ray diffraction studies of cell walls and peptidoglycans from Gram-positive bacteria. Nat New Biol. 1972;235:252–3.
58. Salton MRJ, Kim KS Structure. In: Baron S, editor. Medical Microbiology. 4th ed. Galveston: University of Texas Medical Branch at Galveston; 1996. p. 44–60.
59. Xie J, et al. Crystal structures and antimicrobial and cytotoxic activities of zinc(II), nickel(II) and copper(II) complexes of *N*-(piperidylthiocarbonyl)benzamide. Appl Organomet Chem. 2015;29:157–64.
60. Movahedi E, Rezvani AR. Multispectroscopic DNA-binding studies and antimicrobial evaluation of new mixed-ligand Silver(I) complex and nanocomplex: a comparative study. J Mol Struct. 2018;1160:117–28.
61. Nitha LP, Aswathy R, Mathews NE, Sindhu Kumari S, Mohanan K. Synthesis, spectroscopic characterization, DNA cleavage, superoxidase dismutase activity and antibacterial properties of some transition metal complexes of a novel bidentate Schiff base derived from isatin and 2-aminopyrimidine. Spectrochim Acta Part A. 2014;118:154–61.
62. Mohanan K, Nirmala Devi S, Murukan S. Complexes of Copper (II) with 2-(N-Salicylideneamino)- 3-carboxyethyl-4,5,6,7-tetrahydrobenzo[b]thiophene containing different counter anions. Synth React Inorg Met -Org Chem. 2006;36:441–49.
63. Rafi MU, et al. New pyridazine-based binuclear nickel(II), copper (II) and zinc(II) complexes as prospective anticancer agents. New J Chem. 2016;40:2451–65.
64. Aljahdali MS. Nickel(II) complexes of novel thiosemicarbazone compounds: Synthesis, characterization, molecular modeling and *in vitro* antimicrobial activity. Eur J Chem. 2013;4:434–43.
65. Rigaku. CrysAlisPro. Rigaku Oxford Diffraction. Texas: Rigaku; 2015.
66. Palatinus L, Chapuis G. *SUPERFLIP*—a computer program for the solution of crystal structures by charge flipping in arbitrary dimensions. J Appl Cryst. 2007;40:786–90.
67. Petricek V, Dusek M, Palatinus L. Crystallographic computing system JANA2006: General features. Z Krist. 2014;229:345–52.
68. Rohlicek J, Husak M. *MCE2005*—a new version of a program for fast interactive visualization of electron and similar density maps optimized for small molecules. J Appl Cryst. 2007;40:600–1.
69. DeMarsh, P, Gagnon R, Hertzberg R, Jaworski D Methods of screening for antimicrobial compounds. US patent US20030040032 A1 (2001).
70. Reller LB, Weinstein M, Jorgensen JH, Ferraro MJ. Antimicrobial susceptibility testing: a review of general principles and contemporary practices. Clin Infect Dis. 2009;49:1749–55.
71. Motyl M, Dorso K, Barrett J, Giacobbe R. UNIT 13 A.3 Basic microbiological techniques used in antibacterial drug discovery. Curr Protoc Pharmacol. 2005;13A.3:1–22.
72. Reddy V, Patil N, Angadi S. Synthesis, characterization and antimicrobial activity of Cu(II), Co(II) and Ni(II) complexes with O, N, and S donor ligands. J Chem. 2008;5:577–83.